

# **PART 4**

## **INFRARED ATOMIC PHYSICS AND LINE FORMATION**

# ATOMIC PHYSICS OF THE 12- $\mu\text{m}$ AND RELATED LINES

EDWARD S. CHANG

*Department of Physics and Astronomy, University of Massachusetts,  
Amherst, MA 01003, U.S.A.*

**Abstract.** The 12  $\mu\text{m}$  emission lines were unexpectedly detected about a decade ago. Great progress has been made in understanding the atomic physics underlying these high- $l$  Rydberg transitions in Mg I and other atoms. In a magnetic field, their Landé  $g$  factor is shown to be unity. At disk center, the shift of the absorption trough relative to the emission peak is demonstrated to be due to the quadratic Stark Effect, permitting measurement of the photospheric electric field strengths. Other related lines of Mg I require accurate atomic fine structure data to interpret properly their complex line profiles. Related lines are found in the *ATMOS* spectra for C I, Na I, Al I, Si I, Ca I, and Fe I, in addition to H I.

**Key words:** atomic processes – electric fields – infrared: stars – magnetic fields

## 1. Introduction

The solar 12  $\mu\text{m}$  emission lines were apparently first recorded in 1976 by Goldman *et al.* (1980) in the New Atlas of IR Solar Spectra. However the lines were so startling that they were handmasked in the Atlas, being suspected to be instrumental artifacts. Subsequent observations with a higher resolution instrument at the South Pole, and in a balloon flight, established the authenticity of two 12  $\mu\text{m}$  lines at 811.575 and 818.058  $\text{cm}^{-1}$  and one 7  $\mu\text{m}$  line at 1356.182  $\text{cm}^{-1}$  (Murcray *et al.*, 1981).

Detailed studies of the 12  $\mu\text{m}$  lines were undertaken by Brault and Noyes (1983) at the McMath telescope. Among the many puzzling results were the strong limb brightening, the shift of the absorption trough relative to the emission peak, the Zeeman splitting patterns and the identity of these and of 41 other weaker emission lines. In 1989 the ground-based observations were augmented by the satellite *ATMOS* spectra, which covered the entire 2 to 16  $\mu\text{m}$  range at disk center (Norton and Farmer 1989, Kurucz 1990), adding many more unidentified lines. Most of the stronger lines turned out to be high- $l$  Rydberg lines. The goal of this article is to describe the atomic physics of these lines and to show how to extract from these lines information on the physical properties of the sun.

The 12  $\mu\text{m}$  lines were identified as high- $l$  Rydberg transitions in Mg I, Al I, and Si I (Chang and Noyes, 1983, Chang, 1984), using theory to be reviewed in Section 2. Laboratory verification of the Mg I lines was accomplished by Lemoine, Demuyneck, and Destombes (1988). Further they verified that the Landé factor  $g$  for the two 12  $\mu\text{m}$  lines was unity, as predicted. Magnetic properties of these lines will be explored in Section 3. Deming and collaborators have cleverly exploited the 12  $\mu\text{m}$  lines for vector magnetometry, and he will present his results in these proceedings. Recall that the Mg I 12  $\mu\text{m}$  lines display distinct trough-to-peak shifts. Examination of the *ATMOS* spectra revealed other lines, *e.g.*, at 11  $\mu\text{m}$ , with greater shifts – often in the opposite sense. These shifts were interpreted (Chang and Schoenfeld 1991) as quadratic Stark shifts. In Section 4, the electric properties of these lines will be elucidated. The modeling and formation of these lines in the solar atmosphere have been successfully explained by Chang *et al.* (1991) and by Carlsson *et al.*

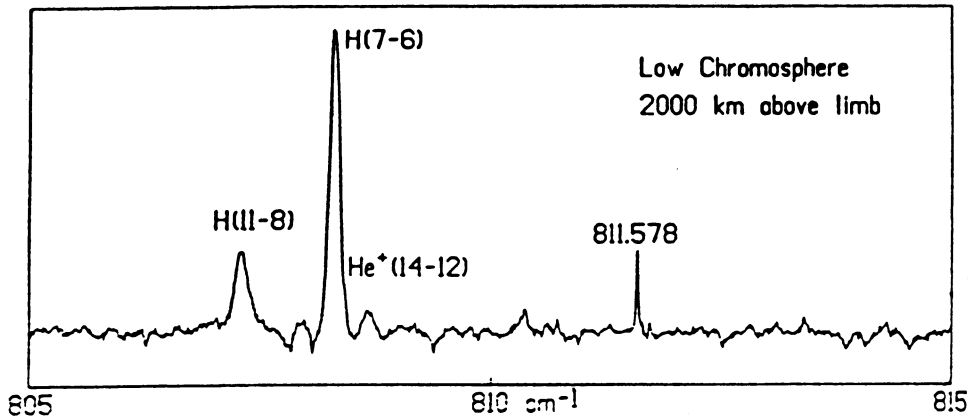


Fig. 1. The 12  $\mu\text{m}$  and the hydrogen lines from Brault and Noyes (1983).

(1992), and are presented separately by Avrett, and by Rutten and Carlsson, in these proceedings.

In addition to the Mg I 12  $\mu\text{m}$  lines, other high- $l$  Rydberg lines are observed at 7 and 11  $\mu\text{m}$ , which also display emission peaks on absorption troughs. Other Mg I lines with intermediate  $l$  and resolvable fine structure have been addressed by Jefferies (1991) as perplexing. All these constitute the related lines of Mg I to be discussed in Section 5. Section 6 delves into the similar lines in other elements. In addition to the fore-mentioned lines of Al I and Si I, newly discovered lines in Fe I are the subject of two poster papers (Johansson *et al.* and Schoenfeld *et al.*, these proceedings). Further lines of C I, Na I, and Ca I have also been identified, but these assignments remain unpublished. In Section 7, I present the conclusions, and prospects for the future.

## 2. High- $l$ Rydberg Atomic Lines

The most important clue to identifying the 12  $\mu\text{m}$  lines is that they lie just on the higher frequency side of the hydrogen  $n = 7$  to 6 line at  $808.283 \text{ cm}^{-1}$  as shown in Figure 1. This immediately suggests that they belong to the 7-6 transition of some other atom, where the levels have very small quantum defects. Such a requirement is automatically met by high- $l$  Rydberg states (where  $l$  is the orbital, and  $n$  the principal, quantum numbers). For then the large centrifugal barrier prevents the Rydberg electron from penetrating the atomic core, which gives rise to the usual quantum defect from short-range interactions. Thus the only contribution comes from the weak long-range interaction which may be regarded as a perturbation on the pure Coulomb potential, responsible for the hydrogen levels. The Rydberg electron's electric field  $E$  induces a dipole moment in the atomic core  $\mu = \alpha E$ , where  $\alpha$  stands for the core's polarizability. The resultant perturbation energy is  $-\mu E$ , which is approximately proportional to  $-\alpha n^{-3} l^{-5}$  (Chang and Noyes 1983). Since

the lower level is perturbed more than the upper, the transition frequency must exceed that of the corresponding hydrogen transition. However, unlike hydrogen, each  $n$  manifold splits into several distinct levels designated by  $l$ , with decreasing energy as  $l$  decreases. The selection rule limits allowed transitions to  $\Delta l = 1$  and  $-1$ , but the former are typically 2 orders of magnitude weaker than the latter, and hence usually unobservable. Recall that the number of radial nodes in the hydrogenic wavefunction is  $n_r = n - l - 1$ . In the  $\Delta l = -1$  case,  $n_r$  is very different for the initial and the final states, resulting in large cancellations in the transition probability. On the other hand,  $n_r$  is identical for the  $\Delta l$  (and  $\Delta n$ ) =  $-1$  transitions, resulting in little cancellation. Indeed for the circular orbits ( $l = n - 1$ ), the nodeless wavefunctions suffer no cancellations at all. Then the transition probability is proportional to  $n^4$ , which is 3 orders of magnitude larger than the typical value for the resonance lines. For the same values of  $n$  but successively lower values of  $l$ , the transition probabilities are weaker by about a factor of two.

These considerations led Chang and Noyes (1983) to identify the 811 and the 818  $\text{cm}^{-1}$  lines as the  $7i-6h$  and the  $7h-6g$  transitions in a neutral atom. The identification was suggested by the large separation which required a value for  $\alpha$  two orders of magnitude greater than for helium. A good candidate was the alkali-like core which, with its lone loose electron, is known for its large polarizability. The first abundant element with such a core is magnesium. Using its known value of  $\alpha$ , we calculated those transition frequencies and found that they agreed well with the observed ones. Additional lines of Mg I were also identified from theory for  $l > 3$ , and from experiment for lower  $l$  levels. Improved theoretical values were given later (Chang 1987).

Laboratory confirmation of the high- $l$  Rydberg lines also came about serendipitously. In measuring the diode-laser spectra of MgH and MgD, Lemoine *et al.* (1988) noted the presence of some atomic Mg I lines. Further studies of the magnesium discharge under high resolution revealed some 30 absorption lines, including the two 12  $\mu\text{m}$  lines. Comparison of laboratory, solar, and theoretical line positions for the high- $l$  Rydberg lines are given in Table 1. Note that the excellent agreement between the positions of the emission peaks and the laboratory data implies that the peaks are essentially unshifted, while the absorption troughs have substantial shifts as will be interpreted in Section 4.

The identification of the emission lines as high- $l$  Rydberg transitions has enormous implications for solar physics. Since these levels are hydrogen-like, their atomic properties are mostly accurately known. This fact greatly facilitates radiative transfer calculations in model atmospheres (Chang *et al.*, 1991; see article by Avrett *et al.*, these proceedings; Carlsson *et al.*, 1992; see article by Rutten and Carlsson, these proceedings). As alluded to earlier, the large opacity of the 12  $\mu\text{m}$  lines is responsible for the greater height of formation, where a small departure from LTE is possible. Thus the rapidly rising line source function in the upper photosphere is responsible for the emission peak and limb brightening. In fact the chromospheric temperature rise has nothing whatsoever to do with the emission lines. Other hydrogen-like properties of these lines will be exploited to measure the magnetic and the electric fields in the solar photosphere next.

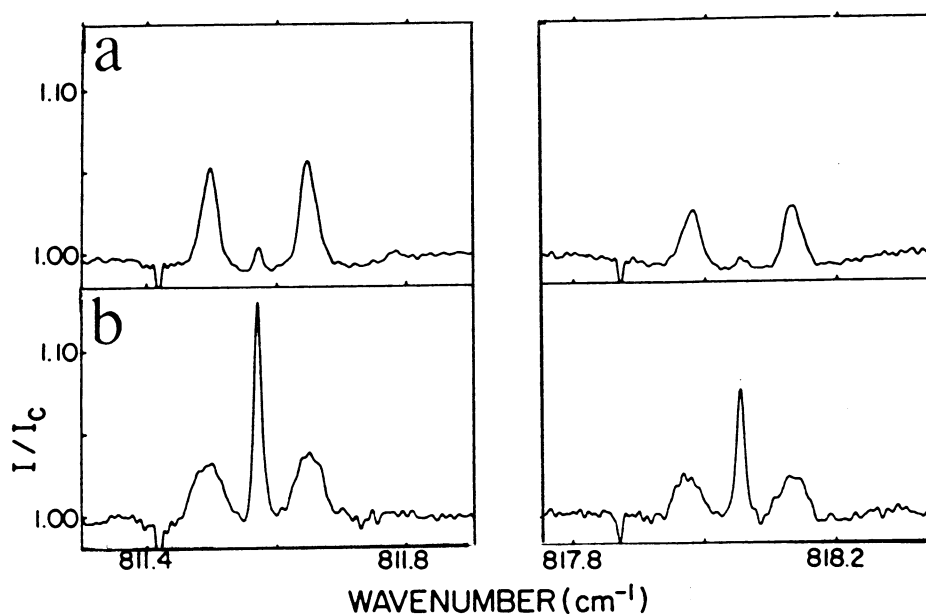


Fig. 2. Penumbra spectrum of the Mg I  $12\ \mu\text{m}$  lines from Brault and Noyes (1983): (a) the  $\sigma$  components in the longitudinal direction; (b) the  $\pi$  component, with twice the strength of the  $\sigma$ , in the transverse direction.

### 3. Magnetic properties

From a simplistic point of view, the Landé  $g$  factor of any high- $l$  Rydberg level is predicted to be unity. First in the absence of a magnetic field, fine structure splittings in the  $12\ \mu\text{m}$  lines have not been observed even in the high resolution diode-laser measurement. Theoretical estimates indicate that they are less than  $0.001\ \text{cm}^{-1}$ , and therefore the spin-orbit coupling must be very weak. Second in the presence of a magnetic field  $B$ , the “classic” interaction with the Rydberg electron exceeds interactions involving the atomic core. Indeed, the  $g$ -factor prediction has been confirmed by diode-laser measurements of the  $\sigma$  components from 200 to 1000 G. The measured  $g$ -factors for the 811 and the 818  $\text{cm}^{-1}$  lines were 0.992(10) and 1.002(10) respectively (Lemoine *et al.*, 1988) – with one standard deviation error in parenthesis.

The penumbral observations of Brault and Noyes (1983) are shown in Figure 2; Figure 2a shows the longitudinal, and Figure 2b the transverse, Zeeman pattern. Without the benefit of line identification, these authors inferred  $g \sim 1$  from some sodium lines, and correctly deduced a measured magnetic field of 1600 G. Recently, exciting measurements of vector magnetic fields using polarimetry of the  $12\ \mu\text{m}$  lines have been carried out by Deming and his collaborators (1988 and these proceedings). For a complete understanding of the magnetic properties of high- $l$  Rydberg

TABLE I  
Observed Mg I Spectral Lines ( $\text{cm}^{-1}$ )

Transition	Solar	Theory <sup>a</sup>	Laboratory <sup>a</sup>
8 <i>h</i> -7 <i>g</i>	530.986	.983	-
7 <i>i</i> -6 <i>h</i>	811.575	.589	.5749(10)
7 <i>g</i> -6 <i>f</i>	848.010	.007	.0109(5)
			.2141(8)
	848.060	.057	.0610(10)
			.0698(7)
9 <i>k</i> -7 <i>i</i>	885.524	.521	.5292(2)
9 <i>i</i> -7 <i>h</i>	886.869	.863	.8717(2)
6 <i>h</i> -5 <i>g</i>	1356.182	.186	-

<sup>a</sup> Integer in column 2 deleted.

lines, one must simultaneously consider internal (magnetic fine structure) and external field effects, as Chang (1987) has done. As long as one of these dominates over the other, the splitting will vary linearly with  $B$ . The case of a strong internal field gives the familiar anomalous Zeeman effect with the splitting proportional to  $g\mu_0 B$ , where the Bohr magneton  $\mu_0$  has the value  $4.67 \times 10^{-5} \text{ cm}^{-1}$  (an erroneous value was given in Chang 1987). For the 12  $\mu\text{m}$  lines, even an external field of 100 G will overwhelm the internal field, resulting in the Paschen-Back effect. Expressions for the splittings and line strengths can be found in Chang (1987). Unfortunately his equation (10b) contained a typographical error in that one of the factors in the numerator should read  $(l \pm m + 2)$ . Thus the relative strength of each  $\sigma$  line when summed over all  $m$  values should be  $1/3$  – the same as for the  $\pi$  line.

#### 4. Electrical Properties

At disk center, the 12  $\mu\text{m}$  lines display an emission peak which agrees with the laboratory line position, and an absorption trough which is shifted. We have undertaken a study of these and some related lines using the *ATMOS* spectra. The troughs for the 811 and 1356  $\text{cm}^{-1}$  lines are shifted to the higher frequency while the 818, 885, and 886  $\text{cm}^{-1}$  lines (see Table 1) are shifted to the lower frequency side. This peculiarity is accounted for by the quadratic Stark effect. In an electric field of strength  $E$ , the energy-level shift is given by  $\delta E_{nl} = -\alpha_{nl} E^2$ , where  $\alpha_{nl}$  stands for the electric dipole polarizability of the Rydberg atom in the state  $nl$ . Its values have been calculated for the transitions of interest by Chang and Schoenfeld (1991). Note that these Rydberg atomic polarizabilities are 4 to 6 orders of magnitude larger than the magnesium core polarizability  $\alpha$ .

To understand the opposite direction of the trough shifts, let us consider the upper levels of the 811 and the 818  $\text{cm}^{-1}$  lines. The 7*i* ( $l = 6$ ) and the 7*h* ( $l = 5$ ) levels are separated by less than 2  $\text{cm}^{-1}$ , and may be regarded as an isolated two-level pair. In the presence of an electric field they admix, and repel each other.

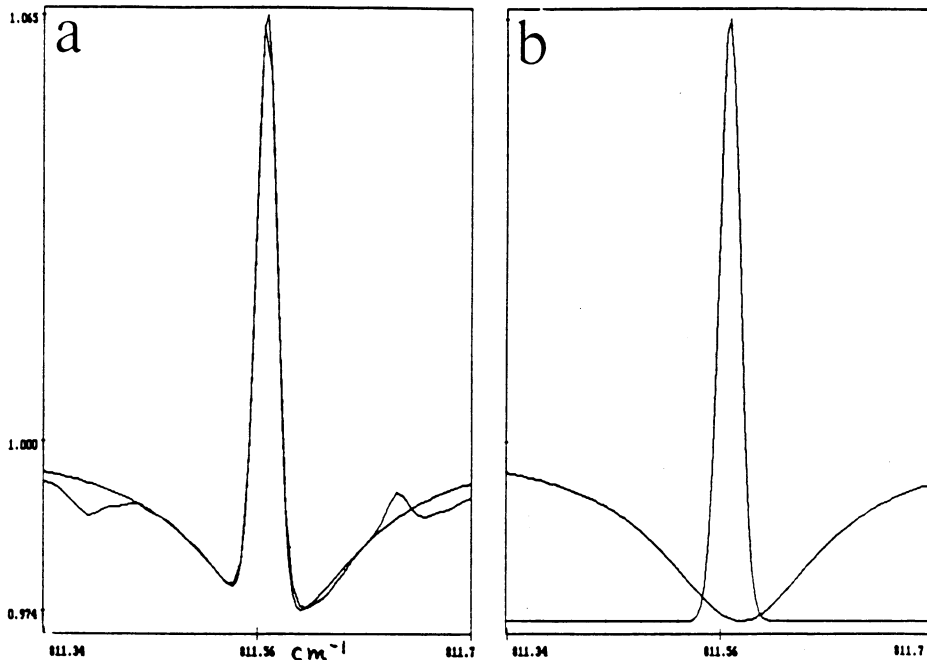


Fig. 3. The  $811\text{ cm}^{-1}$  line profile from Chang and Schoenfeld (1991): (a) The computer-fitted (broken line) and the observed (full line) profiles; (b) The emission peak and the absorption trough.

Therefore the  $7i$  level is shifted upwards ( $\alpha_{7i} < 0$ ) and the  $7h$  level downwards ( $\alpha_{7h} > 0$ ), in agreement with observations. Actually there are two complications which merit further discussion. One is that the  $7h$  level is also repelled upwards by the  $7g$  level. However the  $7g$  level is 3 times further away than the  $7i$  (with about the same off-diagonal matrix element), so the net shift of the  $7h$  level is downwards. The other is that similar shifts occur for the lower levels of the transition. However it can be shown that  $\alpha_{nl}$  varies as  $n^7l^5$ , so the upper level always dominates the shift. Thus we are led to the conclusion that the  $811$  and the  $1356\text{ cm}^{-1}$  lines, whose upper levels are circular states, have absorption troughs shifted towards higher frequency, while the  $818$ ,  $885$ , and  $886\text{ cm}^{-1}$  lines, whose upper levels are not circular, have absorption troughs shifted towards lower frequencies.

Figure 3 shows the  $811\text{ cm}^{-1}$  line at disk center from the *ATMOS* spectra. Panel b shows that the peak has a Gaussian form, and the shifted trough a Lorentzian – as predicted by Chang and Schoenfeld (1991). From the shift of this, and other, lines, we determine electric field strengths of 100 to  $200\text{ V cm}^{-1}$  except for the  $1356\text{ cm}^{-1}$  line which is formed deeper in a stronger electric field.

### 5. Related Lines in Magnesium

So far we have seen that Rydberg lines with  $l > 3$  have negligible fine structure splittings. However lines with  $l = 3$  (or 2) reveal resolvable splittings of a few hundredth  $\text{cm}^{-1}$ . For example, the  $7g-6f$  line (see Table 1) was first observed by Brault and Noyes (1983) at the solar limb as a doublet whose components were of nearly equal intensity and had a spacing of  $0.050 \text{ cm}^{-1}$ . The identification was suspect since the existing atomic data then revealed that the  $6f \ ^1F$  and  $\ ^3F$  were only  $0.03 \text{ cm}^{-1}$  apart and that the intensity ratio should be 1:3. As indicated by the last column of Table 1, the controversy was resolved when high-resolution laboratory data became available. Figure 4 shows that each peak in the solar spectrum was a blend of 2 fine-structure transitions with the  $\ ^3F_2$  blending into the  $\ ^1F_3$  component, thereby yielding nearly equal peaks. Solar modeling of the line showed very good agreement with the observed profiles both at the disk center and at the limb (Chang *et al.*, 1992).

Other related lines involving  $F$  levels in the *ATMOS* data were recently reported by Jefferies (1991). Using the then-current atomic data, he was led to the enigmatic conclusion that the triplets were in emission, while the singlet was in absorption. Using more-recent atomic data, we have computed line profiles from our solar model and have concluded that there is, in fact, no difference between the behavior of triplet and singlet components. Comparison with the observed profiles revealed some subtleties. In the  $6g-5f$  line profile shown in Figure 5, an opacity minimum appeared between the triplet and the singlet emission peaks, all residing in a deep absorption trough. From the observations alone, it is impossible to distinguish the opacity minimum from the fine-structure peaks. In the  $5g-4f$  line at  $2586 \text{ cm}^{-1}$ , our computed profile showed a weak peak for the singlet as for the triplet components. However, the spacing between this peak and the adjacent troughs was less than the *ATMOS* instrumental resolution. Therefore the weak peak disappeared in the observed profile.

The importance of accurate atomic data to the interpretation of solar spectra has just been clearly demonstrated. Fortunately, in Mg I, the recent diode-laser data (Lemoine *et al.*, 1990) and the FTS data (Biémont and Brault, 1986), are available. The high ( $l > 3$ ) Rydberg levels appear to be reliably calculated by theory. Theoretical energies are accurate to within a few thousandths of a wave-number, and their atomic properties are well understood.

### 6. Related Lines in Other Atoms

Since the first identification of the Mg I 12  $\mu\text{m}$  lines, similar high- $l$  Rydberg transitions in other elements were sought and found in the 12  $\mu\text{m}$  window line list. More recently the search has expanded to include the more extensive *ATMOS* data. Hydrogen lines are easily distinguished by their large broadening, due primarily to the linear Stark Effect. These lines become broader and shallower as  $n$  increases. At  $n \sim 10$ , the broadened troughs become indistinguishable from the continuum.

Lines of other atoms are conveniently divided into two categories. One consists of those elements whose atomic cores have an isotropic  $S$  state. Like Mg I, their



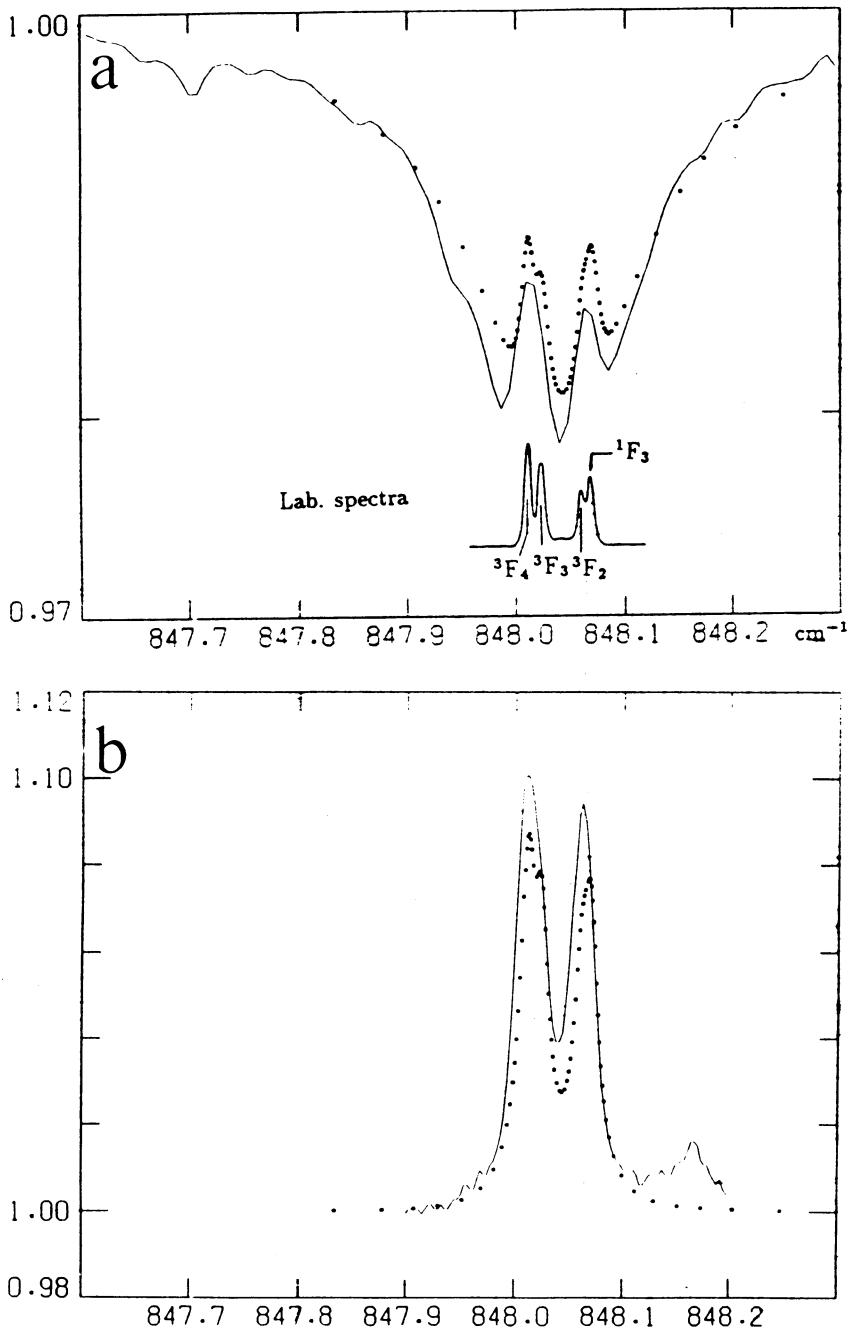


Fig. 4. The Mg I  $7g-6f$  line from Chang *et al.*, (1992). The solid line shows the observations, and the dotted line is the computed profile: (a) at disk center (inset at bottom shows the laboratory spectra); and (b) at the limb.

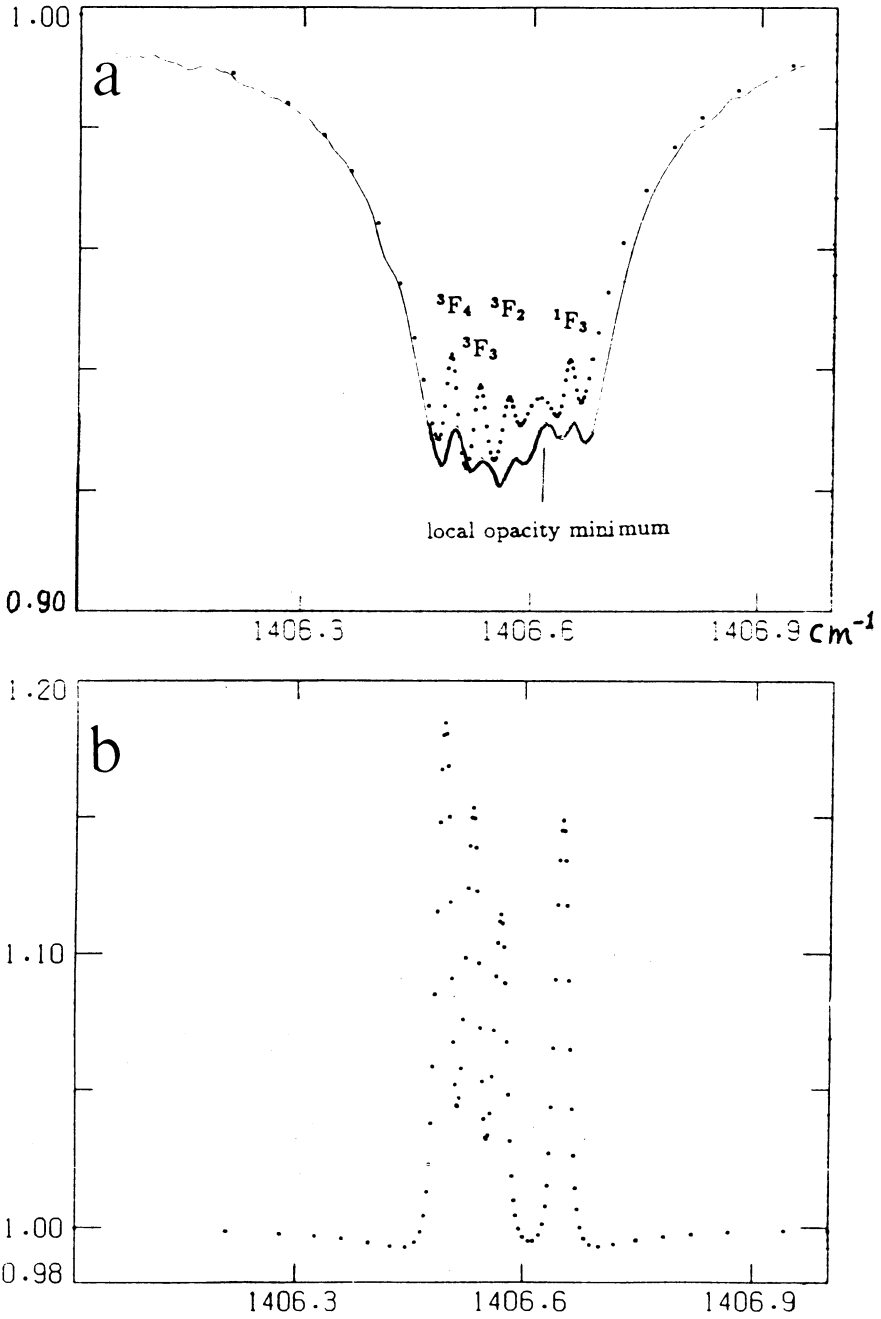


Fig. 5. The Mg I  $6g-5f$  line. The solid line shows the observed, and the dotted line the computed, profiles. Panel (a) refers to the disk center; (b) to the limb.

energy levels are determined by just one parameter, the core polarizability, aside from the trivial reduced-mass Rydberg-constant correction. Some high- $l$  Rydberg lines have been identified for Na I, Al I, and Ca I. They are observed in absorption, with the exception of a few Al I lines which also have weak emission peaks. The other category of lines arise in those atoms whose anisotropic cores have a permanent electric quadrupole moment  $Q$ , in addition to the core polarizability. The electrostatic interaction between  $Q$  and the orbiting Rydberg electron gives rise to a further splitting of each  $nl$  level into sub-levels designated by the  $K$  quantum number. Thus a single Rydberg line in the previous category may fractionate into many lines in these atoms. High- $l$  Rydberg lines in this group have been identified in C I, Si I (Chang 1984), and Fe I (Johansson *et al.*; Schoenfeld *et al.*; these proceedings). Our analysis of the *ATMOS* spectra in the 4, 7, and 12  $\mu\text{m}$  regions reveals no unidentified lines of significant strength. Therefore we do not expect to see high- $l$  Rydberg lines of any other elements.

## 7. Conclusions

In the decade following the discovery of the 12  $\mu\text{m}$  emission lines, great advances have been made in understanding their underlying atomic physics. The hydrogen-like properties of these lines greatly simplify their analysis in the solar spectrum, and enhance the accuracy of the extracted solar properties. As valuable as the 12  $\mu\text{m}$  lines have proven to be for measurements of the solar electric and magnetic fields, it is desirable to explore similar lines in the far infrared. They are formed higher up, reaching into the low chromosphere where little is known about these fields, and in addition the sensitivity increases as the wavelength increases. Consider, for example, the 20  $\mu\text{m}$  line of Mg I which was detected by Brault and Noyes (1983) at the limb. Measurements of this, and other lines, both at the limb and at disk center (and preferably from a satellite) will greatly enhance our knowledge of the astrophysics of the sun.

## Acknowledgements

I thank E. H. Avrett for useful discussions and W. G. Schoenfeld for discussions and assistance in preparation of this manuscript.

## References

- Avrett, E. H., Chang, E. S., and Loeser, R.: 1993, these proceedings.  
 Biémont, E. and Brault, J. W.: 1986, *Physica Scripta* **34**, 751.  
 Brault, J. W. and Noyes, R. W.: 1983, *Astrophys. J. (Letters)* **269**, 61.  
 Carlsson, M., Rutten, R. J., and Shchukina, N. G.: 1992, *Astron. Astrophys.* **253**, 567.  
 Chang, E. S. and Noyes, R. W.: 1983, *Astrophys. J. (Letters)* **275**, 11.  
 Chang, E. S.: 1984, *J. Phys. B* **17**, 11.  
 Chang, E. S.: 1987, *Physica Scripta* **35**, 792.  
 Chang, E. S., Avrett, E. H., Mauas, P. J., Noyes, R. W., and Loeser, R.: 1991, *Astrophys. J. (Letters)* **379**, 79.  
 Chang, E. S., Avrett, E. H., Mauas, P. J., Noyes, R. W., and Loeser, R.: 1992, in M. Giampapa, and J. A. Bookbinder (eds.), *Seventh Cambridge Workshop on Cool Stars, Stellar Systems, and the Sun*, ASP Conference Series, Vol. 26, p. 521.

- Chang, E. S., and Schoenfeld, W. G.: 1991, *Astrophys. J.* **383**, 450.
- Deming, D., Boyle, R. J., Jennings, D. E., and Wiedermann, G. R., : 1988, *Astrophys. J.* **333**, 978.
- Deming D., Hewagama T., and Jennings D. E., McCabe, G., and Wiedemann, G.: 1993, these proceedings.
- Farmer, C. B. and Norton, R. H.: 1989, *A High-Resolution Atlas of the Infrared Spectrum of the Sun and the Earth's Atmosphere from Space*, NASA Ref. Pub. 1224, Vol. 1.
- Goldman, A., Blatherwick, R. D., Murcray, F. H., Van Allen, J. W., Bradford, C. M., Cook G.R., and Murcray D. H.: 1980, *New Atlas of IR Solar Spectra*, Vol. 1, Line Positions and Identifications, Vol.2, The Spectra, Department of Physics, University of Denver.
- Jefferies, J. T.: 1991 *Astrophys. J.* **377**, 337.
- Johansson, S., Nave, G., Geller, M., Sauval, A. J., Grevesse, N.: 1993, these proceedings.
- Kurucz, R.: 1990, in A. N. Cox, W. C. Livingston, and M. Mathews (eds.), *The Solar Atmosphere and Interior*, Tucson, University of Arizona Press, p. 663.
- Lemoine, B., Demuyck, C., Destombes, J. L., and Davis, P. B.: 1988, *J. Chem. Phys.* **89**, 673.
- Lemoine, B., Demuyck, C., and Destombes, J. L.: 1988, *Astron. Astrophys.* **191**, L4.
- Lemoine, B., Petitprez, D., Destombes, J. L., and Chang, E. S.: 1990, *J. Phys. B* **23**, 2217S.
- Murcray, F. J., Goldman, A. Murcray, F. H., Bradford, C. M., Murcray, D. G., Coffey, M. T., and Mankin, W. G.: 1981, *Astrophys. J. (Letters)* **247**, 97.
- Rutten, R., and Carlsson, M.: 1993, these proceedings.
- Schoenfeld, W. G., Chang, E. S., and Geller, M.: 1993, these proceedings.